Article

Current Biology

Synergistic interaction of gut microbiota enhances the growth of nematode through neuroendocrine signaling

Graphical abstract

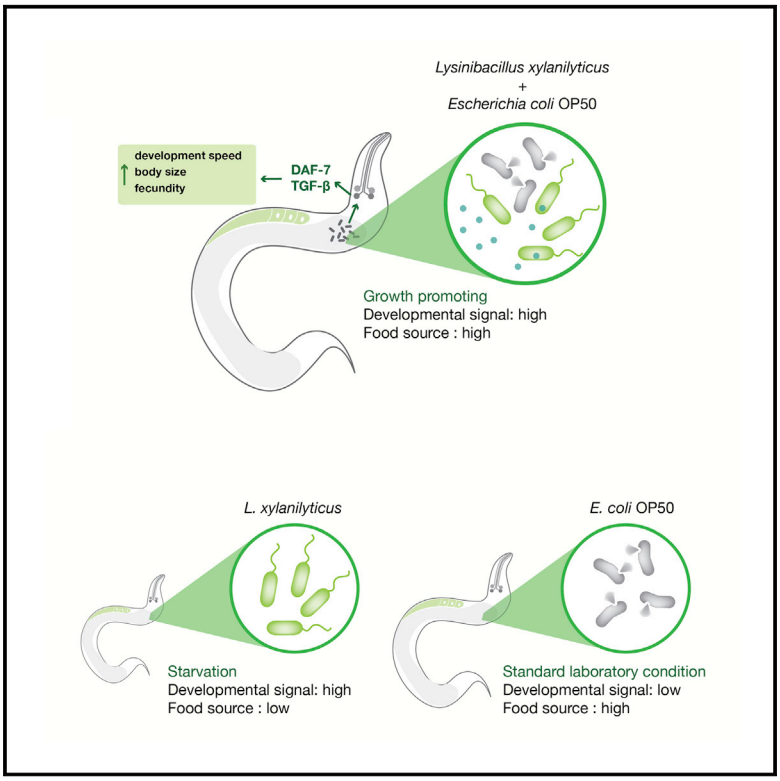

Highlights

- The bacterium *L. xylanilyticus* promotes fitness of its nematode host *P. pacificus*
- *L. xylanilyticus* induces a global transcriptome change in *P. pacificus*
- The host phenotypic changes are regulated by the DAF-7 TGF-β signaling pathway

Authors

Wen-Sui Lo, Ziduan Han, Hanh Witte, Waltraud Röseler, Ralf J. Sommer

Correspondence

ralf.sommer@tuebingen.mpg.de

In brief

Lo et al. find a synergistic interaction between the nematode *P. pacificus* and a member of its gut microbiota. They show that the combination of *E. coli* and a member of nematodes' natural microbiota *L. xylanilyticus* increase the fitness of *P. pacificus* via induction of the neuroendocrine peptide of *P. pacificus*.

Lo et al., 2022, Current Biology *32*, 1–14
May 9, 2022
https://doi.org/10.1016/j.cub.2022.03.056

CellPress

Current Biology

CellPress

Article

Synergistic interaction of gut microbiota enhances the growth of nematode through neuroendocrine signaling

Wen-Sui Lo,[1] Ziduan Han,[1] Hanh Witte,[1] Waltraud Röseler,[1] and Ralf J. Sommer[1,2,*]
[1]Max Planck Institute for Biology, Department for Integrative Evolutionary Biology, Max-Planck-Ring 9, Tuebingen, 72076, Germany
[2]Lead contact
*Correspondence: ralf.sommer@tuebingen.mpg.de
https://doi.org/10.1016/j.cub.2022.03.056

SUMMARY

Animals are associated with a diverse bacterial community that impacts host physiology. It is well known that nutrients and enzymes synthesized by bacteria largely expand host metabolic capacity. Bacteria also impact a wide range of animal physiology that solely depends on host genetics through direct interaction. However, studying the synergistic effects of the bacterial community remains challenging due to its complexity. The omnivorous nematode *Pristionchus pacificus* has limited digestive efficiency on bacteria. Therefore, we established a bacterial collection that represents the natural gut microbiota that are resistant to digestion. Using this collection, we show that the bacterium *Lysinibacillus xylanilyticus* by itself provides limited nutritional value, but in combination with *Escherichia coli*, it significantly promotes life-history traits of *P. pacificus* by regulating the neuroendocrine peptide in sensory neurons. This gut-to-brain communication depends on undigested *L. xylanilyticus* providing *Pristionchus* nematodes a specific fitness advantage to compete with nematodes that rupture bacteria efficiently. Using RNA-seq and CRISPR-induced mutants, we show that 1-h exposure to *L. xylanilyticus* is sufficient to stimulate the expression of *daf-7*-type TGF-β signaling ligands, which induce a global transcriptome change. In addition, several effects of *L. xylanilyticus* depend on TGF-β signaling, including olfaction, body size regulation, and a switch of energy allocation from lipid storage to reproduction. Our results reveal the beneficial effects of a gut bacterium to modify life-history traits and maximize nematode survival in natural habitats.

INTRODUCTION

Gut microbiota influence host physiology in diverse ways, including development, nutrition, immunity, and behavior.[1] However, studying the molecular mechanisms that mediate these effects remains challenging primarily due to the sheer complexity of bacteria communities. To this end, invertebrate model organisms, such as nematodes and fruit flies, are valuable systems to study host-microbe interactions for multiple reasons. In comparison with vertebrate model organisms that harbor thousands of bacterial species, many invertebrate gut microbiota are composed of relatively simple communities of bacteria.[2,3] In addition, gnotobiotic animals can easily be generated through sterilization protocols, and in the case of nematodes, many species can be cultured on monoxenic diets under laboratory conditions.[4] When combined with well-developed genomic resources and molecular toolkits, nematodes provide traceable systems to investigate the causation of microbiome impacts.

Free-living, bacterivorous nematodes thrive on decomposing organic matter, where they interact with a high density of bacterial populations.[5,6] Recently, the characterization of the nematode-associated microbial community provided a valuable foundation to investigate the function of the natural microbiome on nematode life-history traits, primarily in the model organisms *Caenorhabditis elegans* and *Pristionchus pacificus*.[7–11] For example, vitamins and amino acids synthesized by naturally associated bacteria were shown to influence development and growth and to change nematode behavior.[12–15] Yet it is largely unknown if these bacteria benefit nematodes through means other than serving as food sources. In addition, while the nematodes harbor a diverse gut microbiota, if and how the bacterial interspecies interaction shapes host physiology is currently little understood.

The nematodes *P. pacificus* and *C. elegans* have an estimated evolutionary divergence of 100 million years.[16] *P. pacificus* is a soil nematode with a worldwide distribution and is often found in close association with scarab beetles as dauer larvae, a dormant stage.[17] Nematodes resume development after the death of the beetle and start feeding on bacteria that thrive on the insect carcass in the soil (Figure 1A). This tripartite system of insect-nematode-bacteria was recently studied in greater detail and provided a new prospect for analyzing nematode-bacteria interactions. Specifically, the rhinoceros beetle *Oryctes borbonicus* from La Réunion Island in the Indian ocean is an ideal model system, as it shows a *P. pacificus* association in more than 90% of all beetle individuals at several locations.[18] The succession and dynamics of

Please cite this article in press as: Lo et al., Synergistic interaction of gut microbiota enhances the growth of nematode through neuroendocrine signaling, Current Biology (2022), https://doi.org/10.1016/j.cub.2022.03.056

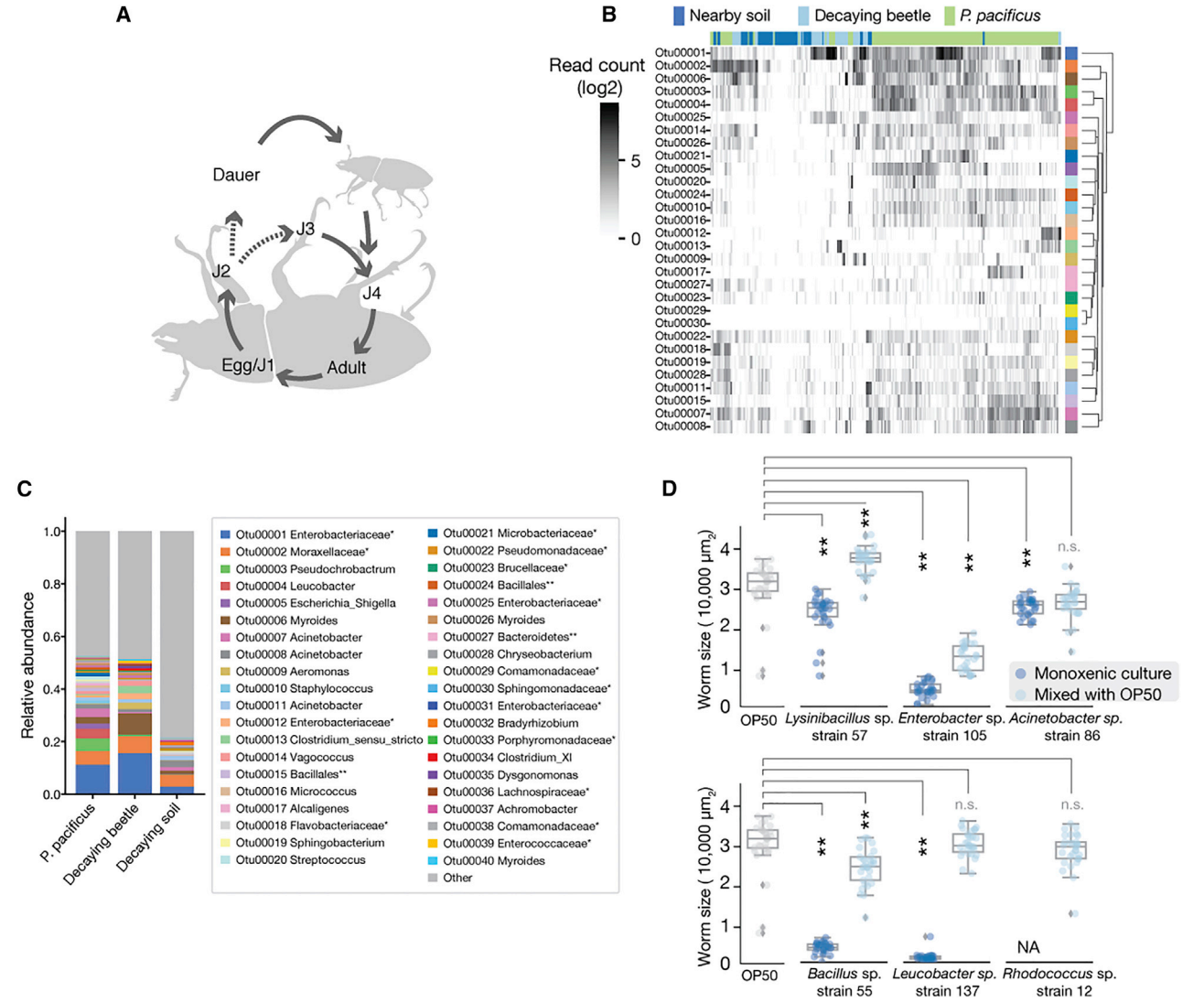

Figure 1. Characterization of the *P. pacificus* gut microbiota

(A) Schematic illustration of the *P. pacificus* life cycle. First-stage (J1) juveniles stay in the egg so that second-stage (J2) juveniles hatch. Under favorable environmental conditions, animals undergo a direct life cycle and progress through the J3 and J4 stages to become adults. Under unfavorable environments, nematodes form dauer larvae and disperse.

(B) Heatmap indicates the microbiota composition profiles of *P. pacificus* collected from beetle carcasses (green), decaying beetles (cyan), and nearby soil (blue). Samples (row) and OTUs (columns) were clustered based on similarity using hierarchical clustering analysis. Colors of the column indicate the taxonomy of OTUs as shown in (C) and the complete OTUs are listed in Data S1.

(C) The frequency of OTUs of pooled samples. OTUs were assigned to each bacterial genus or to family (*) and order (**) if the genus-level classification could not be assigned.

(D) The effect of gut microbiota on *P. pacificus* body size. Nematodes were grown on monoxenic cultures or mixed cultures of the tested bacterium and *E. coli* OP50 (mixed culture). Body size of *P. pacificus* was measured at the late J4 stage (54 h after synchronization). Note that most animals were lost on *Rhodococcus* sp. 012 bacterial lawn because of the avoidance behavior of the nematode.

One-way ANOVA with Tukey HSD test is used to compare body size differences between *E. coli* OP50 and the tested bacterial culture. n.s., non-significant; *$p < 0.05$, **$p < 0.005$. See also Data S1.

nematodes and the composition of the microbiota of the decaying beetle have been characterized over a 12-week period.[10,11] These studies revealed that the nematode exhibits a biphasic boom and bust dynamics that are largely dependent on bacterial load. The nematode gut microbiota are more similar to that of the beetle than the one of the surrounding soil. Also, there is unexpected conservation of the taxonomic composition of the microbial community over the 3 months of succession.[11] It is important to note that the beetle carcasses harbor bacterial populations that are different from those of the decaying fruits and plant materials that inhabit *C. elegans*.[7–9] Together, these studies provide an ecological framework for mechanistic studies on host-microbe interactions.

Please cite this article in press as: Lo et al., Synergistic interaction of gut microbiota enhances the growth of nematode through neuroendocrine signaling, Current Biology (2022), https://doi.org/10.1016/j.cub.2022.03.056

Compared with *C. elegans*, *P. pacificus* exhibits two important morphological differences that have strong consequences with regard to bacterial interactions and feeding in general. First, *Pristionchus* and all other members of the Diplogastridae family have lost the grinder, an organ in the pharynx that mechanically breaks open bacterial cells.[19] Second, they develop teeth-like denticles in their mouth, which allow predatory feeding on other organisms to supplement their bacterial diet.[20,21] The absence of the grinder and the limited efficiency of the digestive system result in live bacterial cells accumulating inside the intestinal lumen.[22] As a result, it has long been known that bacteria can pass completely through the *Pristionchus* gut alive.[23] These morphological differences alter the interaction between bacteria and the host and result in striking adaptive changes of nematode immunity. For example, *P. pacificus* is resistant to the nematode pathogen *Bacillus thuringiensis*, whose virulence against *C. elegans* is mediated by the release of exotoxins following the lysis of bacterial cells.[24,25] The ingested, but not digested, bacteria can have distinct interactions with *P. pacificus* compared with *C. elegans*.[25] Thus, differences in the morphology of the feeding structures and the ecological niches may shape the host-microbe interactions of *P. pacificus* and *C. elegans*. Therefore, the *P. pacificus*-microbiota system provide a potential opportunity to reveal novel host-microbe interactions.

In this study, we aimed to elucidate a beneficial nematode-bacterium interaction and the underlying molecular mechanisms. We isolated *P. pacificus* from beetle carcasses and established a collection of their gut microbiota. We found that the bacterium *Lysinibacillus xylanilyticus* on its own provides limited nutrition, but the combination with *Escherichia coli* OP50 promotes life-history traits of *P. pacificus*, including growth, developmental speed, and brood size. We show that the growth-promoting effects depend on undigested and live *L. xylanilyticus*, and the mechanism is conserved among nematodes without the functional grinder. We focused on the nematode response and demonstrated that the *L. xylanilyticus*-induced phenotypic changes were regulated by two paralogs of *daf-7*, the nematode-specific ligand of the transforming growth factor-β pathway (TGF-β). We analyzed the influence of *L. xylanilyticus* on TGF-β signaling through CRISPR/Cas9-induced mutants and showed how the microbiota changes host gene expression and physiology. Together, our study shows that the synergistic interaction of the gut bacteria provides *P. pacificus* the signal to grow.

RESULTS

Culture-based and 16S rRNA-based community profiling reveals dominant species of the *P. pacificus* gut microbiota

To investigate the function of the *P. pacificus* gut microbiota and identify potential beneficial interactions, we established a collection of bacteria isolated from their natural habitat. Specifically, *P. pacificus* nematodes were sampled from the decaying rhinoceros beetles *Oryctes borbonicus*, and their gut microbiota were isolated. In total, we obtained 118 bacterial isolates of 29 different genera as living cultures. Among them, 63 isolates belonged to six species that represent the dominant bacteria, including *Lysinibacillus* sp., *Enterobacter* sp., *Acinetobacter* sp., *Bacillus* sp., *Leucobacter* sp., and *Rhodococcus* sp. To test whether our culture-based approach successfully isolated the dominant populations of *P. pacificus* gut microbiota, we re-analyzed the 16S rDNA amplicon sequences collected from the same natural habitat in previous years.[10] As shown in Figures 1B and 1C, the *P. pacificus* gut microbiota is dominated by the phyla Proteobacteria, Bacteroidetes, Actinobacteria, and Firmicutes with a community structure that is distinct from the one of the surrounding soil and the decaying beetle. The species mentioned above belong to the dominant phyla Proteobacteria, Actinobacteria, and Firmicutes, revealing a similar dominance pattern in the 16S rRNA-based community profiling. The consistency in the composition of the bacterial community, despite that they were collected in different years, indicates that the structure of the *P. pacificus* gut microbiota is stable and reproducible.

Interactions between *P. pacificus* and its gut microbiota range from beneficial to pathogenic

Next, we examined the effects of representative bacterial isolates on *P. pacificus* by measuring their impact on the growth of the animals. We randomly selected one isolate from each of the six dominant species for testing. When grown on monoxenic cultures of these bacteria, we observed various effects on *P. pacificus* in comparison with animals grown on the standard food source *E. coli* OP50 (Figure 1D). Specifically, nematodes (1) were arrested as second-stage juveniles (J2) (*Enterobacter* sp. 105, *Bacillus* sp. 055, and *Leucobacter* sp. 137), (2) had a slower development speed (*Lysinibacillus* sp. 057 and *Acinetobacter* sp. strain 86), or (3) escaped from the culture plate (*Rhodococcus* sp. 012). Thus, in monoxenic cultures, all six bacteria had negative effects on nematode growth and development.

To test whether these effects are due to a poor nutritional quality (e.g., difficulty to be digested) or the pathogenicity of the bacteria, we grew nematodes in mixed cultures that contained *E. coli* OP50 and the bacterium subject to be tested with an initial ratio of 9:1 (henceforth referred to as "mixed bacteria" or "mixed cultures"). Intriguingly, the supplementation with *E. coli* completely eliminated the negative effects of *Leucobacter* sp. 137 and *Rhodococcus* sp. 012 and strongly reduced the effect of *Bacillus* sp. 055. Thus, the negative effect caused by these bacteria on *P. pacificus* is largely compensated by adding *E. coli*. Likely, these bacteria did not represent suitable food sources and cause nematode starvation, whereas the supplementation with *E. coli* overcame these limitations. In contrast, *P. pacificus* still exhibited a smaller body size on *Enterobacter* sp. 105 and *E. coli* mixed cultures, suggesting a pathogenic interaction. Surprisingly, however, *P. pacificus* showed a significant increase in body size when grown on mixed cultures of *Lysinibacillus* sp. 057 and *E. coli* OP50 (Figure 1D). Together, these findings suggest that gut microbiota can have strong, but different, effects on nematode growth.

L. xylanilyticus serves as poor food but promotes fitness in combination with *E. coli*

We focused on *Lysinibacillus* sp. 057 to investigate the growth-promoting effects triggered by gut microbiota. The isolate 057 was identified as *Lysinibacillus xylanilyticus* based on its phylogenetic placement (Figure S1), a gram-positive bacterium

Please cite this article in press as: Lo et al., Synergistic interaction of gut microbiota enhances the growth of nematode through neuroendocrine signaling, Current Biology (2022), https://doi.org/10.1016/j.cub.2022.03.056

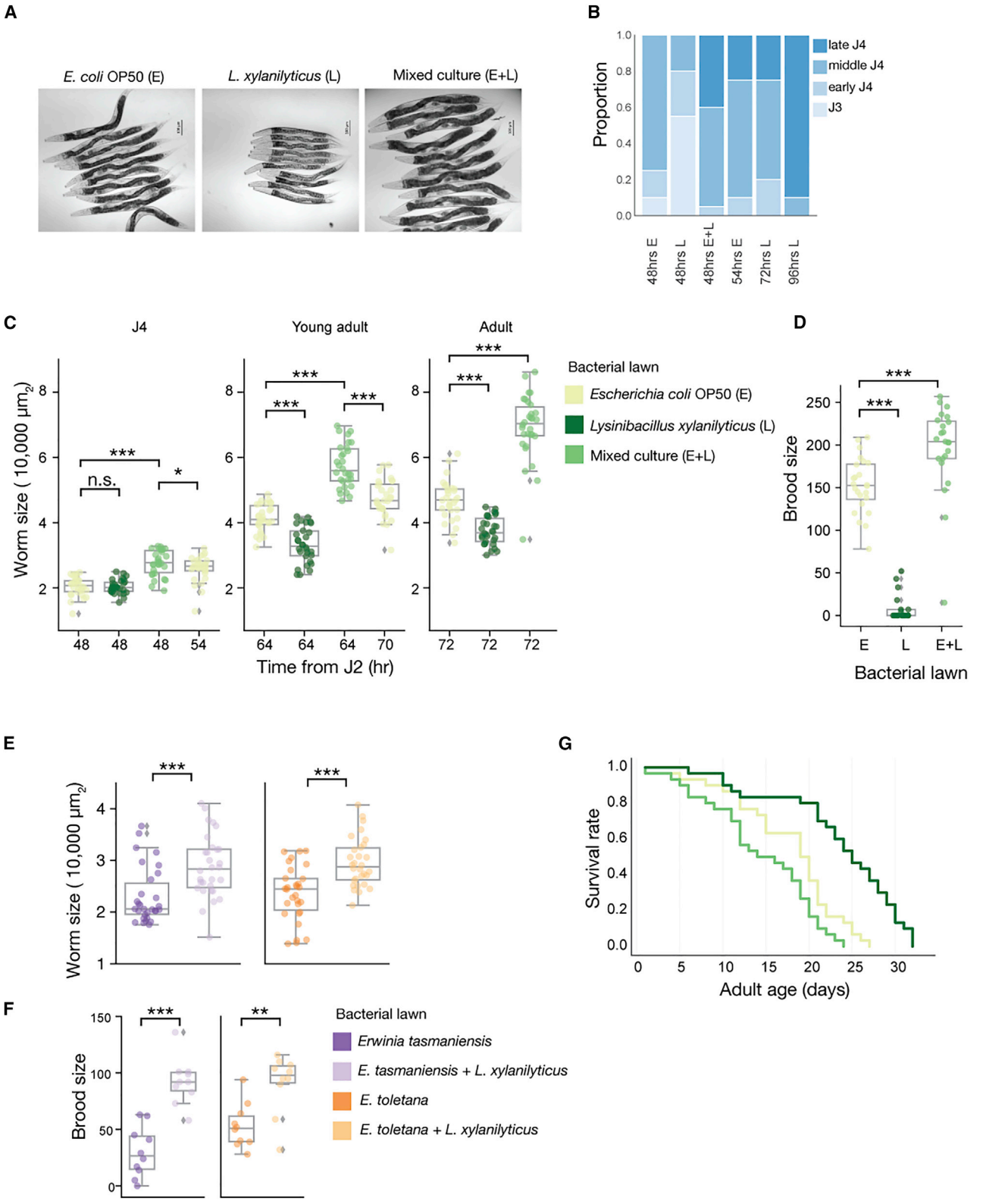

Figure 2. *L. xylanilyticus* and *E. coli* OP50 mixed cultures promote fitness of *P. pacificus*

(A) Representative images of young adults grown on different bacterial cultures. Synchronized nematodes grown on three different bacterial cultures for 64 h were photographed. Scale bars, 100 μm.

(B) Developmental progression on three different bacterial cultures. E, monoxenic *E. coli* culture; L, monoxenic *L. xylanilyticus* culture; E + L, mixed culture.

(legend continued on next page)

commonly associated with organic matter-enriched environments.[26] To better understand how *L. xylanilyticus* affects its nematode host, we measured *P. pacificus* life-history traits on monoxenic cultures of *L. xylanilyticus*, *E. coli* OP50, and on mixed cultures. Concomitant to the smaller body size (Figure 2A), *P. pacificus* development was slower when grown on *L. xylanilyticus* monoxenic cultures (Figure 2B). For example, 48 h after synchronization, most animals on *L. xylanilyticus* were in the J3 or early J4 juvenile stage, whereas animals on *E. coli* were mostly at the middle of the J4 stage. In contrast, a substantial fraction of animals on a mixed culture have reached the late J4 juvenile stage (Figure 2B). It took 54 h on *E. coli* for *P. pacificus* to reach J4, whereas 72 h for nematodes on *L. xylanilyticus* to reach J4. When we investigated animal size at these respective time points, we found significant differences at time points from 48, over 64–72 h (Figure 2C). These findings indicate that *L. xylanilyticus* affect developmental speed and nematode size in all postembryonic stages. Finally, hermaphrodites were capable of producing eggs on all three culture conditions; however, most of the eggs did not hatch when *P. pacificus* was grown on *L. xylanilyticus* monoxenic culture, resulting in very small brood sizes (Figure 2D). In contrast, a mixed culture significantly increased brood size relative to a monoxenic culture of *E. coli* (Figure 2D).

To test whether *L. xylanilyticus* provides beneficial effects when cocultured with bacteria other than *E. coli*, we cocultured *L. xylanilyticus* with the naturally associated isolates *Erwinia tasmaniensis* NA6 and *E. toletana* V100,[27] which belong to the most abundant Enterobacteriaceae family on the beetle carcass (Figure 1C). We found that the combination of *L. xylanilyticus* with these two bacteria showed similar growth and fecundity-promoting effects (Figures 2E and 2F), suggesting that these synergistic interactions can occur in natural habitats.

Besides development and fecundity, the bacterial cultures also affect nematode lifespan (Figure 2G). The *L. xylanilyticus* monoxenic culture has a longevity-promoting effect, which is likely caused by dietary restriction. In contrast, on a mixed culture, *P. pacificus* exhibits the shortest lifespan of all three tested conditions, which may result from a trade-off between fecundity and lifespan.[28] Together, our results indicate that *L. xylanilyticus* in combination with *E. coli* affects all four tested life-history traits of *P. pacificus*: nematodes develop faster, grow to larger body size, and produce more offspring, but with the cost of reducing longevity.

Intestinal localization of live *L. xylanilyticus* induces a growth-promoting effect

Bacterial species of the Bacillaceae family are not part of the core gut microbiota in *C. elegans*.[7,9,29] To test whether the effects of *L. xylanilyticus* are conserved among bacterivorous nematodes, we included *C. elegans* N2 into our analysis. In contrast to *P. pacificus*, *C. elegans* N2 has a comparable body size on monoxenic *E. coli* OP50 and *L. xylanilyticus* cultures. We only observed a moderate increase in body size and growth rate in mixed cultures (Figures 3A, S2A, and S2C). To test whether mechanical rupture of *L. xylanilyticus* by the grinder is responsible for the difference between the two bacterivorous nematodes, we used *C. elegans phm-2*, a grinder dysfunctional mutant that can accumulate live bacteria in the intestine.[30] Intriguingly, *C. elegans phm-2* showed a decrease in body size on monoxenic *L. xylanilyticus* cultures and an increase in body size, brood size, and developmental speed on the mixed bacterial culture, similar to *P. pacificus* (Figures 3A and S2A–S2C).

To visualize the localization of bacterial cells, we used an *E. coli* OP50 derivative that expresses DsRed protein as an indicator for bacterial localization. In *P. pacificus*, *E. coli* OP50::DsRed cells were lysed as indicated by the diffused fluorescence signal in the intestine (Figure 3B). In contrast, intact *L. xylanilyticus* cells were accumulating in the intestinal lumen of *P. pacificus* (Figure 3C). In *C. elegans*, we did not find bacterial cells in the intestine of wild-type animals (Figure S2D). However, in *phm-2* mutants, both intact *E. coli* and *L. xylanilyticus* were observed (Figure 3D).

Next, we tested if the bacterial cells localized in the *P. pacificus* intestine are viable by measuring their transcriptional activity.[31] Surprisingly, transcription from *E. coli* was barely detectable in either monoxenic or mixed cultures (Table S1), suggesting that most of the *E. coli* was digested and its RNA degraded. In contrast, we detected ~16-fold more RNA-seq reads of *L. xylanilyticus* than that of *E. coli* in mixed cultures (Table S1). Note that *L. xylanilyticus* comprised 10% of the starting population of bacteria and approached 25% after 48 h of incubation on NGM plates (Figure S3A). Thus, at this time point, *E. coli* was still three times more abundant on NGM agar plates, suggesting that digestion rather than outgrowth by *L. xylanilyticus* was responsible for the 16-fold abundance of *L. xylanilyticus* in the *P. pacificus* intestine.

Finally, to test whether the growth-promoting effect requires the metabolic activity of *L. xylanilyticus*, we adopted the recently developed paraformaldehyde (PFA)-treatment protocol that kills bacterial cells but maintains their nutritional value.[32] For that, live *E. coli*- and PFA-treated *L. Xylanilyticus* cells were mixed at ratios of 9:1 and 1:1, respectively. Interestingly, PFA-treated *L. Xylanilyticus* lost the effect on body size at a ratio of 9:1 (*E. coli*-PFA-treated *L. Xylanilyticus*) (Figure 3E). We only detected a mild growth-promoting effect at a ratio of 1:1 However, this increase is significantly smaller than the increase in growth of nematodes on mixed cultures containing live *L. Xylanilyticus* (Figure 3E). These results suggest that live *L. Xylanilyticus* colonizing the intestinal lumen is essential for the growth-promoting effect, whereas the nutritional value released from PFA-killed bacteria plays only a minor role.

(C) Nematode body size on three different bacterial cultures at 48 (middle J4), 64 (young adult), and 72 (adult) h. Note that animals grow faster on mixed cultures. Therefore, we included additional time points on *E. coli* OP50, 54 (late J4), and 70 (adult) h to compare developmental stages.
(D) Brood size on three bacterial cultures.
(E and F) The effects of mixed culture of naturally associated *Erwinia* spp. and *L. xylanilyticus* on *P. pacificus* body size and brood size.
(G) *P. pacificus* longevity on the three bacterial culture conditions.
All statistical tests are t tests with an adjective p value using the false discovery rate (FDR). n.s., non-significant, *$p < 0.05$, **$p < 0.005$, ***$p < 0.0005$. See also Figure S1.

Please cite this article in press as: Lo et al., Synergistic interaction of gut microbiota enhances the growth of nematode through neuroendocrine signaling, Current Biology (2022), https://doi.org/10.1016/j.cub.2022.03.056

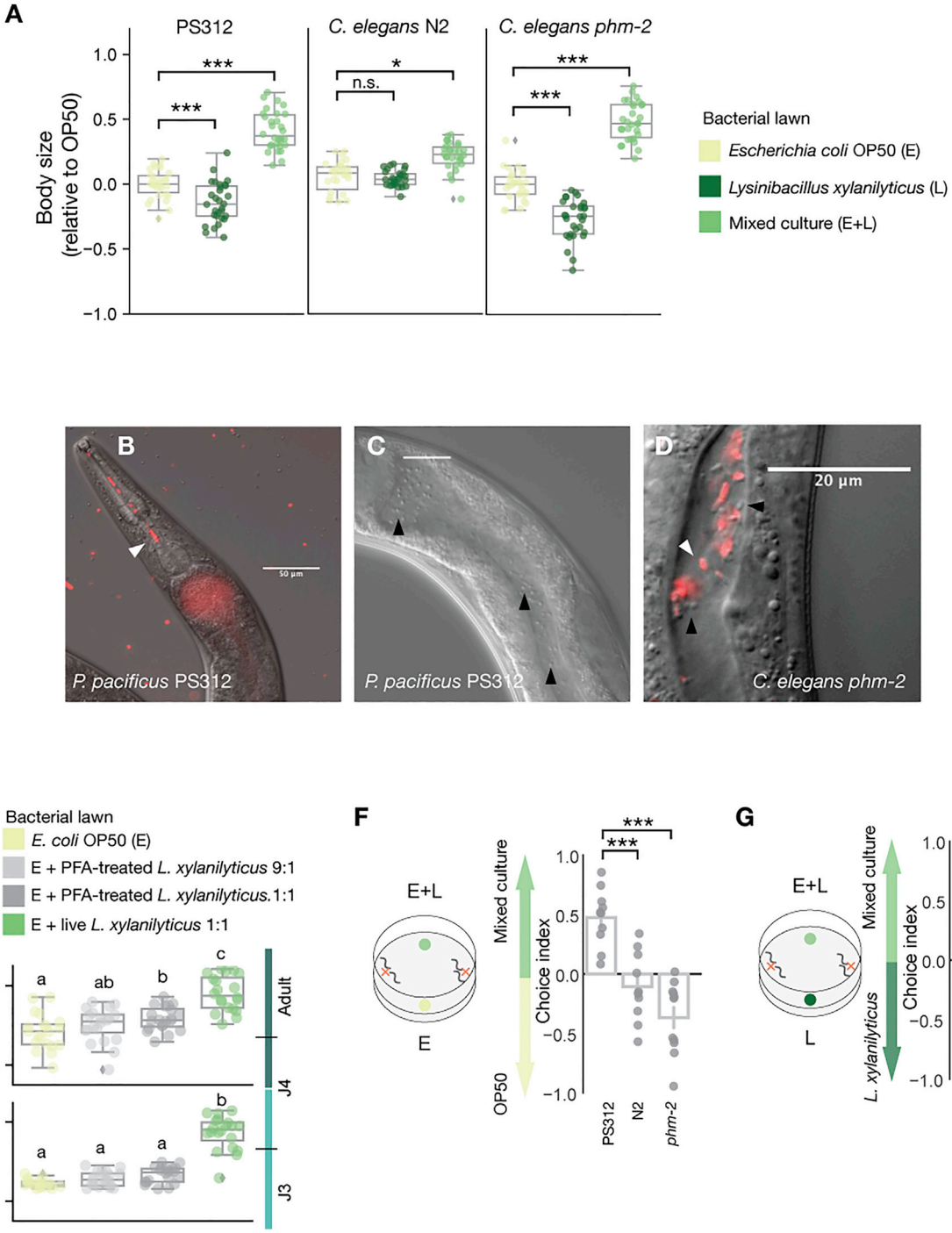

Figure 3. *L. xylanilyticus* has species-specific effects on nematodes

(A) Relative body size of *P. pacificus* wild-type PS312, *C. elegans* wild-type N2, and the *C. elegans* grinder mutant *phm-2* at 54 h after synchronization. Body size was normalized by the median value of body size on *E. coli* OP50 of each strain, respectively.

(B–D) Microscopic images of the nematode intestinal localization of *E. coli* OP50 expressing DsRed (white triangle) and *L. xylanilyticus* (black triangle).

(B) *E. coli* OP50 was lysed in the intestine of *P. pacificus*. Scale bars, 50 μm.

(C) Intact *L. xylanilyticus* cells are accumulating in the intestinal lumen of *P. pacificus*. Scale bars, 20 μm.

(D) Intact *E. coli* OP50 and *L. xylanilyticus* in the intestine of *C. elegans phm-2*. Scale bars, 20 μm

(E) Effect of paraformaldehyde (PFA)-treated and live *L. xylanilyticus* on the body size of *P. pacificus* PS312. Nematodes were exposed to different bacterial lawns for 24 h from J3 to middle J4 (bottom) and J4 to adult (top). Labels indicate the treats are belonging to the same statistical group after one-way ANOVA with Tukey HSD test.

(legend continued on next page)

Please cite this article in press as: Lo et al., Synergistic interaction of gut microbiota enhances the growth of nematode through neuroendocrine signaling, Current Biology (2022), https://doi.org/10.1016/j.cub.2022.03.056

P. pacificus is attracted to *L. xylanilyticus*, but *C. elegans* is not

To further decipher the host-bacterial relationship, we performed chemotaxis assays to measure the nematodes' olfactory preference between *L. xylanilyticus* and *E. coli*. Between a mixed culture and *E. coli*, *P. pacificus* strongly preferred the mixed culture, whereas neither *C. elegans* N2 nor the *phm-2* mutant did (Figure 3B). These findings indicate that *P. pacificus* and *C. elegans* have distinct preferences for *L. xylanilyticus* (Figure 3B). In addition, *P. pacificus* was indifferent toward mixed cultures when offered an *L. xylanilyticus* monoxenic culture as an alternative (Figure 3C). These results suggest that the odor of *L. xylanilyticus* plays a major role to attract *P. pacificus*.

L. xylanilyticus induces global transcriptional changes, including key genes in the TGF-β signaling pathway

Next, we performed RNA-seq to detect the gene expression changes induced by *L. xylanilyticus*. We included, besides the *P. pacificus* wild-type PS312, two *P. pacificus* strains, RSB068 and RSB080, that were recently collected from La Réunion Island to avoid possible effects from long-term laboratory adaptation. To detect early response genes to *L. xylanilyticus*, synchronized *P. pacificus* J2 larvae were grown on *E. coli* and switched to mixed bacterial cultures for 1, 4, and 24 h, respectively, before RNA extraction (Figure 4A). Surprisingly, a 1-h exposure to *L. xylanilyticus* was sufficient to trigger global expression changes of *P. pacificus*. In total, 1,053 and 3,211 genes were differentially expressed at 1 and 24 h, respectively. Subsequently, we performed gene set enrichment analysis (GSEA) to identify the biological processes that were altered by *L. xylanilyticus*. Gene sets related to protein kinases and phosphatases were significantly enriched (Figure 4B; Data S2A and S2B), which may regulate the downstream pathways and contribute to the observed global transcriptome and phenotypic changes. In addition, genes associated with larval development, gonad development, and cell cycle regulation were also found to be enriched (Data S2C and S2D). Finally, in the KEGG gene sets, genes associated with carbohydrate, lipid, and amino acid metabolism were significantly enriched (Figure 4B; Data S2E and S2F), suggesting a reprogramming of energy metabolism.

Intriguingly, our transcriptomic analyses revealed that two homologs of *C. elegans daf-7* were differentially expressed after the 1-h exposure to mixed cultures in *P. pacificus* (Figure 4C). *Cel-daf-7* encodes a TGF-β ligand, a member of a highly conserved signal transduction pathway.[33,34] As both genes show sequence homology to the single *Cel-daf-7* genes, we have designated these genes as *Ppa-daf-7.1* and *Ppa-daf-7.2* following standard nomenclature rules. In *C. elegans*, two major TGF-β pathways exist: the DBL-1 pathway controlling body size, male tail morphology, and innate immunity (TGF-β Sma/Mab), whereas the DAF-7 pathway regulates the switch between direct and indirect (dauer) development (TGF-β dauer). These two pathways are also known to regulate aging and longevity, reproduction, chemosensation, and lipid metabolism.[35] The predicted components of these two pathways in *P. pacificus* are illustrated in Figure 4D. Note that in contrast to *Ppa-daf-7.1* and *Ppa-daf-7.2*, the central genes of the DBL-1 TGF-β pathway, insulin/IGF-1 signaling (IIS) pathway, and the target of rapamycin (TOR) signaling pathways, which act as regulators of growth and metabolic responses to a variety of internal and environmental stimuli in *C. elegans*,[36,37] were not differentially expressed. These results suggest a crucial role of DAF-7-mediated signaling for *L. xylanilyticus*-mediated growth promotion.

Ppa-daf-7.1/2 are expressed in two amphid neurons on both bacterial diets

In *C. elegans*, *daf-7* expression is sensitive to bacterial diets. Specifically, *Cel-daf-7* is expressed in the ASI pair of amphid neurons when fed on *E. coli*[33,34] but expands its expression to ASI and ASJ neurons in response to the pathogen *Pseudomonas aeruginosa* PA14.[38] To characterize the homologs of *daf-7* in *P. pacificus*, we generated transcriptional reporter lines carrying a *Ppa-daf-7.1*p::GFP and *Ppa-daf-7.2*p::TurboRFP, respectively. Interestingly, when grown on *E. coli*, both *daf-7* genes were expressed in two pairs of amphid neurons (Figure 4E), which are likely to be AM10/ASI and AM8/ASJ.[39] When grown on mixed bacteria, the intensity of the fluorescence signals increased, but the cells in which both genes were expressed remained the same (Figure 4E). Thus, the duplication of *daf-7* in *P. pacificus* and their different expression patterns on *E. coli* suggest diverged regulatory mechanisms.

L. xylanilyticus-induced transcriptomic changes are regulated by TGF-β signaling

To investigate the function of *daf-7* and other genes in the TGF-β pathway in the *P. pacificus-L. xylanilyticus* interaction, we generated CRISPR/Cas9-derived mutants in several TGF-β pathway genes. Specifically, we knocked out *Ppa-daf-7.1*, *Ppa-daf-7.2*, *Ppa-daf-4*, *Ppa-daf-8*/R-Smad, and *Ppa-sma-2*/RSmad (Figure 4D). The first four genes are orthologs of the TGF dauer pathway, whereas *Ppa-sma-2* is included to examine the role of the TGF-β Sma/Mab pathway. We obtained mutants in all five targeted genes that result in frameshift mutations and are likely loss-of-function or strong reduction-of-function alleles (Figure S4).

We first monitored the expression profiles in the DAF-7 pathway mutants relative to *P. pacificus* wild-type animals using the same experiential design as described in Figure 4A. We estimated the similarity of gene expression between mutants by calculating Pearson's correlation coefficients between the expression profiles on mixed bacteria and *E. coli* for all mutants. Wild-type *P. pacificus* animals showed changes in gene expression on the mixed bacteria that were increased over time (Figure 5A). We found that the expression profiles of the two *daf-7* single mutants on mixed bacteria also changed but were different from that of wild-type animals (Figure 5A). In contrast,

(F and G) Chemotaxis behavior varies between *P. pacificus* and *C. elegans* strains. The bacterial choice assay was set up as indicated in the cartoon. Nematodes had the choice between *E. coli* OP50 and a mixed culture (F) or *L. xylanilyticus* and a mixed culture (G). E, monoxenic *E. coli* culture; L, monoxenic *L. xylanilyticus* culture; E + L, mixed culture.

Statistical tests in (A), (F), and (G) are t tests with an adjective p value using the false discovery rate (FDR). n.s., nonsignificant; *$p < 0.05$, **$p < 0.005$, ***$p < 0.0005$. See also Figure S2.

Please cite this article in press as: Lo et al., Synergistic interaction of gut microbiota enhances the growth of nematode through neuroendocrine signaling, Current Biology (2022), https://doi.org/10.1016/j.cub.2022.03.056

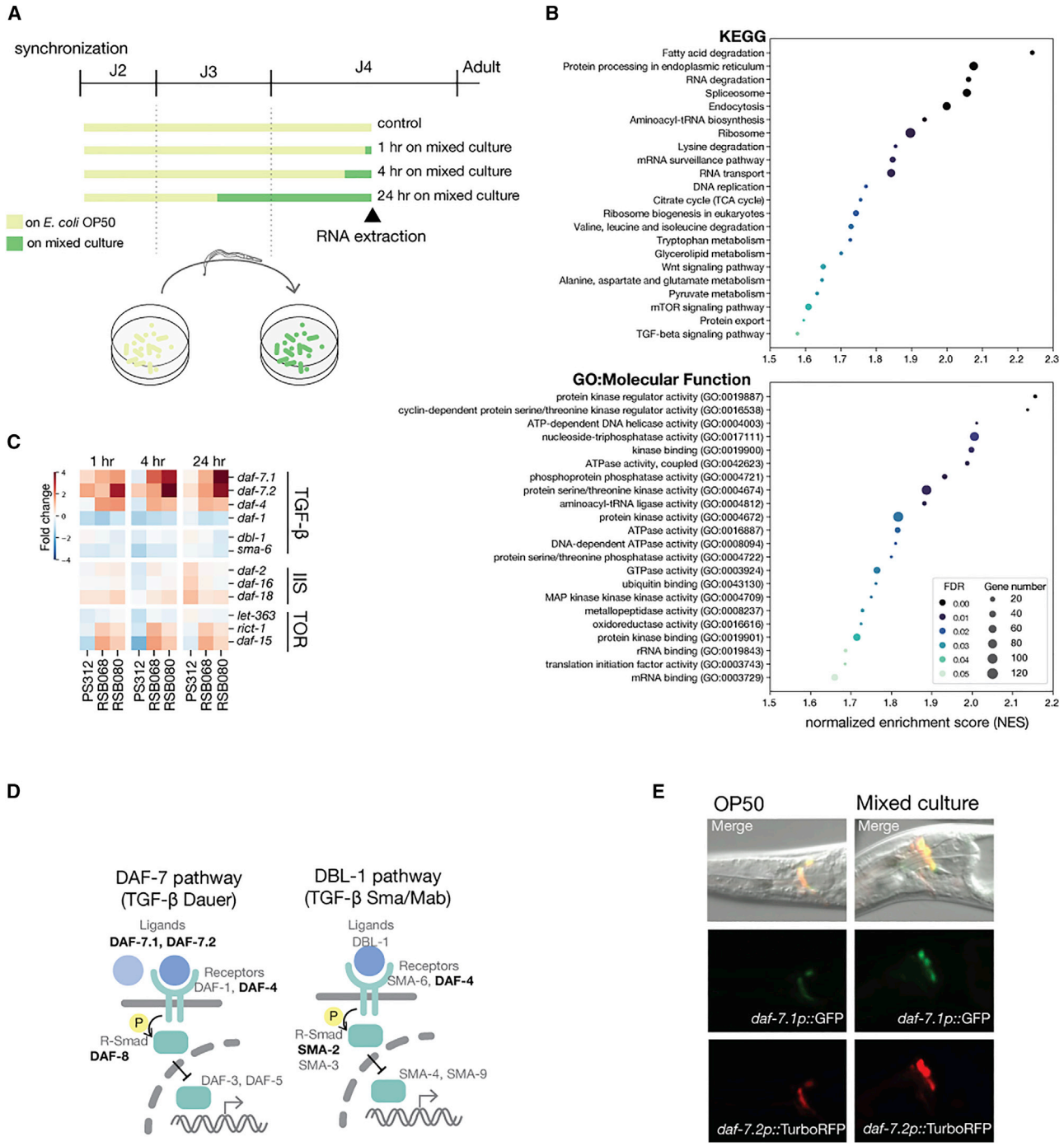

Figure 4. *L. xylanilyticus* induces global transcriptional changes, including key genes in the TGF-β signaling

(A) Schematic of experimental design. *P. pacificus* was first grown on *E. coli* OP50 and switched to mixed cultures for different periods of time before RNA extraction.

(B) Plots showing normalized enrichment scores (NESs) of the gene set enrichment analysis (GSEA) from KEGG (top) and GO Molecular Function (bottom). The comparisons between 1 h on the mixed culture and *E. coli* OP50 are shown.

(C) Heatmap of the gene expression fold changes between *E. coli* OP50 and mixed cultures in three *P. pacificus* strains at different time points. Selected genes of the TGF-β signaling, insulin/IGF-1 signaling (IIS), and target of rapamycin (TOR) pathways are shown. The expression of *daf-7.1* in *P. pacificus* PS312 was measured using qRT-PCR (Figure S3) because of its low expression.

(D) Canonical TGF-β signaling pathway in *P. pacificus*. TGF-β pathway mutants examined in this study are highlighted in bold.

(E) Representative images of *daf-7.1*p::GFP and *daf-7.2*p::TurboRFP gene expression in *P. pacificus* on *E. coli* OP50 (left) and mixed cultures (right).

See also Data S2 and Figures S2 and S3.

Please cite this article in press as: Lo et al., Synergistic interaction of gut microbiota enhances the growth of nematode through neuroendocrine signaling, Current Biology (2022), https://doi.org/10.1016/j.cub.2022.03.056

CellPress

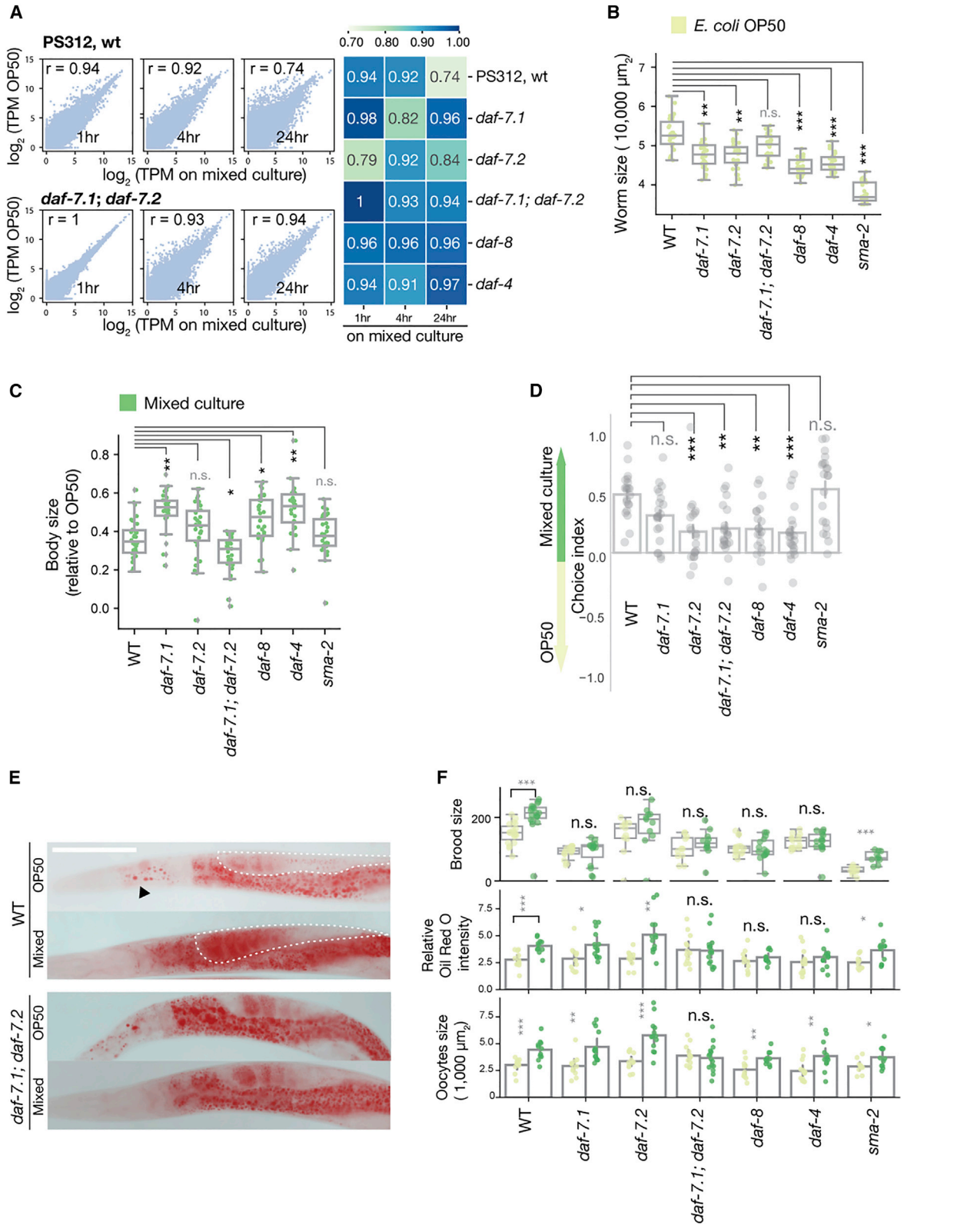

(legend on next page)

Please cite this article in press as: Lo et al., Synergistic interaction of gut microbiota enhances the growth of nematode through neuroendocrine signaling, Current Biology (2022), https://doi.org/10.1016/j.cub.2022.03.056

Ppa-daf-7.1 Ppa-daf-7.2 double mutants, as well as *Ppa-daf-4* and *Ppa-daf-8* single mutants, lost the response to the mixed bacterial culture and remained similar to the expression profiles on an *E. coli* diet (Figure 5A). These results support the idea that the TGF-β dauer pathway plays a central role in the response to *L. xylanilyticus* and the induction of phenotypic changes in *P. pacificus*.

L. xylanilyticus-induced body size increase is partially controlled by TGF-β signaling

Next, we tested if the body size increase triggered by *L. xylanilyticus* is regulated by TGF-β signaling. In general, TGF-β mutants have a smaller body size when grown on *E. coli* (Figure 5B). While the DBL-1 pathway mutant *Ppa-sma-2* shows the strongest effect, single mutants of the DAF-7 pathway also show a significantly reduced body size on *E. coli*. This result is different from the corresponding mutants in *C. elegans*.[40] Note, however, that *Ppa-daf-7.1 Ppa-daf-7.2* double mutants show a weaker body size effect than single mutants, which suggests compensatory mechanisms. To study if the exposure to mixed cultures compensated for the small-body size effect, we analyzed the normalized dataset relative to *E. coli* (Figure 5C). Indeed, the *Ppa-daf-7.1 Ppa-daf-7.2* double mutants showed a significantly reduced response to the mixed bacteria relative to wild type. However, DAF-7 pathway single mutants displayed a significant increase in body size relative to wild-type animals. In contrast, the DBL-1 pathway was not involved in body size regulation on mixed cultures. Together, these results suggest that body size increase induced by *L. xylanilyticus* requires complex genetic regulation and is at least partially dependent on *Ppa-daf-7* signaling, including positive and negative regulatory interactions (Figures 5C and S5A). Strikingly, genome analysis indicates several expansions of DAF-7 pathway genes in *P. pacificus* (see below).

Next, we wanted to know whether TGF-β pathway mutants interfere with the *P. pacificus* olfactory profiles toward mixed cultures. When nematodes were given a choice between *E. coli* and mixed cultures, we found that *Ppa-daf-7.1 Ppa-daf-7.2* double mutants, as well as *Ppa-daf-4* and *Ppa-daf-8* single mutants, reduced the preference toward the mixed cultures (Figure 5D). In contrast, the *Ppa-sma-2* mutant showed a chemotaxis profile similar to wild-type animals. However, to rule out that the observed chemotaxis phenotypes are due to a complete absence of olfaction in these mutant backgrounds, we wanted to test whether TGF-β pathway mutants were still able to choose between the supernatant and cell pellets of *E. coli* OP50. As for wild-type animals, mutant strains also preferred the odor of the supernatant indicating that olfaction is still intact (Figure S5B). Thus, chemotaxis toward *L. xylanilyticus* is dependent on the canonical *Ppa*-DAF-7 pathway (Figure 5D).

L. xylanilyticus changes lipid metabolism and reproduction through DAF-7 TGF-β signaling

Our RNA-seq results indicated a switch in energy allocation when *P. pacificus* was grown on the mixed bacteria. Specifically, genes for fatty acid degradation were significantly enriched (Figure 4B). We performed Oil Red O staining to monitor lipid droplet distribution of *P. pacificus* on different bacterial cultures. On *E. coli*, *P. pacificus* wild-type animals accumulated large amounts of lipid droplets in intestinal and epidermal cells, while the exposure to mixed bacterial culture dramatically reduced the lipid droplets in epidermal cells. Instead, the intensity of Oil Red O in the gonad was significantly increased (Figure 5E). Concomitantly, we found that the size of the gonadal arms also increased (Figure 5E), a finding that may contribute to the larger brood size observed on mixed cultures (Figure 2D). Reproduction is an energetically costly process and it has been suggested that nematodes experience a trade-off between reproduction and fat storage.[41] In natural habitats, nematodes must detect environmental conditions and choose between reproduction and energy storage accordingly to maximize their survival chances. Our results suggest that the presence of *L. xylanilyticus* may represent a favorable environment and stimulate the reproduction of *P. pacificus*.

Finally, we tested if the regulation of reproduction and fat storage are mediated by the DAF-7 pathway. All of the mutants in the *Ppa*-DAF-7 pathway lost their response in brood size, but not the mutant in the *Ppa*-DBL-1 pathway (Figure 5F). As TGF-β mutants displayed defects in egg laying, we also measured the size of the gonadal arms instead of brood size. The *Ppa-daf-7.1 Ppa-daf-7.2* double mutant lost its response to *L. xylanilyticus* in lipid droplet relocation and gonad development (Figure 5F). Similarly, the *Ppa-daf-4* and *Ppa-daf-8* mutants also lost their response to *L. xylanilyticus* in lipid droplet relocation, but the size of gonads was increased. Our results support the role of *Ppa-daf-7.1/2* for the *L. xylanilyticus*-induced increase in reproduction and lipid metabolism. Yet it is likely that additional interactions between TGF-β and other signaling pathways are of importance for the regulation of these physiological traits. Taken together, our results demonstrate that the *Ppa*-DAF-7 pathway, but not

Figure 5. The effect of *L. xylanilyticus* is dependent on the TGF-β pathway

(A) Scatterplots showing the transcriptome comparison of *P. pacificus* wild type and *daf-7* double mutant grown on *E. coli* OP50 and 1, 4, or 24 h on mixed cultures. *r* indicates the Pearson correlation coefficient of transcriptomic profiles. The correlation coefficients between *E. coli* OP50 and mixed cultures of all TGF-β pathway mutants are summarized in the heatmap.

(B) Body size of *P. pacificus* wild-type PS312 and TGF-β mutants on *E. coli* OP50.

(C) Relative body size of *P. pacificus* PS312 and TGF-β mutants on mixed culture. The body size was normalized by the median value of body size on OP50 of each strain. Synchronized adult animals were used (72 h after synchronization). The p values between the body size of wild-type and TGF-β mutants on the mixed culture are shown.

(D) Chemotaxis behavior of *P. pacificus* wild-type (WT) and TGF-β mutant nematodes.

(E) Representative pictures of Oil Red O-stained *P. pacificus*. Scale bars, 100 μM. Triangles mark the lipid droplet at the pharynx. Dashed lines indicate the anterior oocytes.

(F) Brood size (top), relative Oil Red O signal intensity (middle), and the size (lower) of the anterior oocyte of wild-type (WT) and TGF-β pathway mutants.

All statistical tests are against wild type. One-way ANOVA with Tukey HSD test was used to compare body size differences and chemotaxis behavior. t test was used to compare brood size, Oil Red O intensity, and oocyte size. n.s., nonsignificant, *$p < 0.05$, **$p < 0.005$, ***$p < 0.0005$. See also Figure S5.

Please cite this article in press as: Lo et al., Synergistic interaction of gut microbiota enhances the growth of nematode through neuroendocrine signaling, Current Biology (2022), https://doi.org/10.1016/j.cub.2022.03.056

CellPress

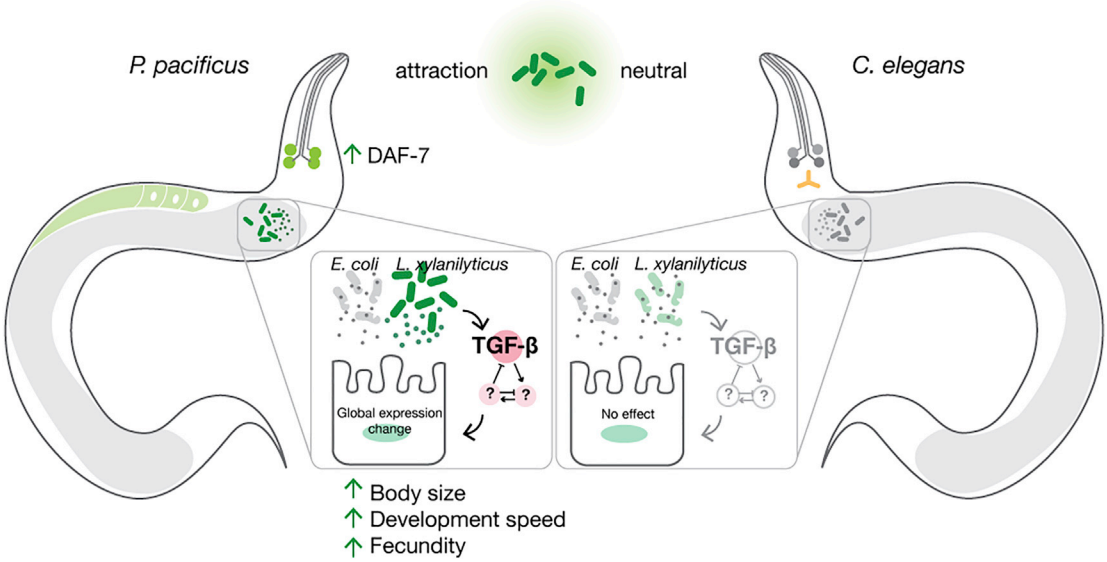

Figure 6. Model for nematode-*L. xylanilyticus* interaction

In *P. pacificus*, the metabolically active *L. xylanilyticus* combined with the lysed *E. coli* stimulated the expression of the two copies of *daf-7*. In *C. elegans*, *L. xylanilyticus* served as the food source and has no effect on the nematode host.

Ppa-DBL-1 pathway, is required for the fecundity-associated energetic trade-off induced by *L. xylanilyticus*.

DISCUSSION

In unstable or unpredictable environments, such as the microbial community on the soil organic matter that *P. pacificus* and *C. elegans* rely on, fast reproduction and high fecundity are favored by natural selection.[11,42,43] Here, we demonstrate that the combination of the natural gut bacterium *L. xylanilyticus* with *E. coli* OP50 (but also natural *Erwinia* ssp.) increases the developmental speed and fecundity of *P. pacificus*. This species-specific interaction provides *P. pacificus* a better chance to outgrow other nematodes in the same habitat. Although it is not exclusive, several of the changes on *P. pacificus* described in this study depend on DAF-7/TGF-β signaling, which is known to play a central role in the regulation of physiological responses. To the best of our knowledge, this is the first study in nematodes that demonstrates a bacterium of the natural gut microbiota to promote the growth of the host through neuroendocrine signaling.

While the hosts harvest bacterial nutrients through digestion, the beneficial interactions can be produced by viable bacterial cells that are resistant to digestion. In *Drosophila*, for example, the growth-promoting *Lactobacillus* is constantly lysed by the host immune response in the intestine.[44] Interestingly, the compound of crosstalk is a byproduct of bacterial fermentation rather than nutrients released through cell digestion.[45,46] Remarkably, in this study, we show a beneficial nematode-microbes interaction that resulted from the divergent functions of ingested bacteria (Figure 6). In *P. pacificus*, the majority of *E. coli* cells were lysed and used as a major nutritional source, while most *L. xylanilyticus* cells remained viable and metabolically active in the intestine. In *C. elegans* N2, in contrast, with a larger part of bacterial cells being digested, we detected relatively mild growth-promoting effects. However, it is noteworthy that *P. pacificus* grown on *L. xylanilyticus* monoxenic cultures could still reach adulthood, suggesting that some of them are digested. In addition, our previous studies showed that not all *E. coli* cells are disrupted during the passage of the gut.[20] Thus, the comprehensive identification of the bacterial components and metabolic network will be required to further decipher the mechanisms of the *E. coli-L. xylanilyticus-P. pacificus* interaction.

The TGF-β pathway is conserved throughout the animal kingdom and plays a role in various cellular functions. However, the DAF-7 pathway is nematode specific and less conserved.[47] It has been speculated that the rapid evolution of TGF-β ligands may be associated with the adaptation to different environments, such as the evolution from the free-living to the parasitic lifestyle.[47] In *P. pacificus*, *daf-7* was duplicated and it displayed a different expression from *C. elegans* when fed on *E. coli* OP50. We speculate that these evolutionary alterations in *daf-7* expression among free-living nematodes are likely in response to the diverse microorganisms they encounter.

In addition to the TGF-β pathway, IIS and TOR pathways are known to transduce nutritional signals to the metabolism and development of invertebrate animals. In *Drosophila*, the gut microbiota regulate the systemic growth of the host through the IIS[45] and TOR[48] pathways. In *C. elegans*, the IIS and TOR share roles with TGF-β to regulate dauer development, growth, and fat metabolism. These three pathways are known to interact with each other.[35–37] It is noteworthy that some components are diversified between *C. elegans* and *P. pacificus* and copy number variations resulting from lineage-specific gene duplication events exist. For example, more than one homolog of *daf-3*, *daf-4*, and *daf-7* in *P. pacificus* have been identified (El Paco gene annotations V3; http://pristionchus.org/). In addition, *C. elegans* has around 40 insulin-like peptides (ILPs),[36] yet less

than 10 ILPs homologs have been identified in *P. pacificus* (El Paco gene annotations V3; http://pristionchus.org/). The duplicated TGF-β components and the ILPs may act to compensate for the response to *L. xylanilyticus* in *P. pacificus daf-7* mutants, but this hypothesis awaits future studies. A survey to identify components of TGF-β and IIS pathways should help to better understand the mechanisms of *P. pacificus-L. xylanilyticus* interaction.

Finally, our studies support the notion that the natural microbiome is necessary to comprehensively understand the physiological responses of model organisms. In mice, for example, natural gut bacteria have been collected from wild populations and introduced to laboratory mice to better recapitulate the physiology outside the laboratory.[49,50] Given that all nematodes have co-evolved with natural microorganisms for millions of years, different physiological and behavioral phenotypes are expected when nematodes are cultured on natural bacteria and combinations thereof. Indeed, around 30% of the annotated protein-coding genes in *P. pacificus* are not expressed when *E. coli* is used as the only food source,[51] and the function of these genes may need to be studied in a natural context. Similarly, in *C. elegans*, recent studies suggest that the intestinal localization of bacteria is commonly found in the wild,[7–9] whereas under laboratory conditions, this is only a marginal phenomenon. Consequently, a synthetic bacterial community derived from *C. elegans* habitats has been established to better study nematode physiology in the context of natural microbiota.[52] Taken together, our results demonstrate that the *P. pacificus*-beetle system is a valuable resource to establish the natural microbiota-based models to study the microbiota-related mechanisms and will provide valuable resources to investigate the host-microbe evolution.

STAR★METHODS

Detailed methods are provided in the online version of this paper and include the following:

- KEY RESOURCES TABLE
- RESOURCE AVAILABILITY
  - Lead contact
  - Materials availability
  - Data and code availability
- EXPERIMENTAL MODEL AND SUBJECT DETAILS
  - *P. pacificus* and *C. elegans* Strains
  - Bacterial Culture
- METHOD DETAILS
  - Bacteria Collection and Identification
  - Quantification of Microbial Communities
  - *L. xylanilyticus* Whole-genome Sequencing and Phylogenetic Analysis
  - Paraformaldehyde Treatment of *L. xylanilyticus*
  - Chemotaxis Assay
  - RNA Sequencing and Data Analysis
  - Generation of Transgenic Animals
  - Generation of P. pacificus TGF-β Pathway Mutants by CRISPR/Cas9
  - qRT-PCR and qPCR
- QUANTIFICATION AND STATISTICAL ANALYSIS

SUPPLEMENTAL INFORMATION

Supplemental information can be found online at https://doi.org/10.1016/j.cub.2022.03.056.

ACKNOWLEDGMENTS

We thank members of our La Réunion team for the field sampling, especially Dr. Matthias Herrmann and Christian Weiler. We thank Dr. Adrian Streit, Dr. Christian Feldhaus, and Veysi Piskobulu for the protocol of Oil Red O staining and visualization. Z.H. was supported by a Humboldt Research Fellowship for postdoctoral researchers. This work was funded by the Max Planck Society.

AUTHOR CONTRIBUTIONS

Conceptualization, W.-S.L. and R.J.S.; methodology, W.-S.L. and Z.H.; investigation, W.-S.L., Z.H., H.W., and W.R.; writing – original draft, W.-S.L.; writing – review & editing, R.J.S. and Z.H.; formal analysis, W.-S.L.; funding acquisition, R.J.S.; supervision, R.J.S.

DECLARATION OF INTERESTS

The authors declare no competing interests.

Received: October 12, 2021
Revised: February 23, 2022
Accepted: March 18, 2022
Published: April 8, 2022

REFERENCES

1. Gilbert, J.A., Blaser, M.J., Caporaso, J.G., Jansson, J.K., Lynch, S.V., and Knight, R. (2018). Current understanding of the human microbiome. Nat. Med. *24*, 392–400.
2. Newton, I.L.G., Sheehan, K.B., Lee, F.J., Horton, M.A., and Hicks, R.D. (2013). Invertebrate systems for hypothesis-driven microbiome research. Microbiome. Sci. Med. *1*, 1–9.
3. Petersen, J.M., and Osvatic, J. (2018). Microbiomes in natura: Importance of invertebrates in understanding the natural variety of animal-microbe interactions. mSystems *3*, e00179–17.
4. Wood, W.B. (1988). The nematode *Caenorhabditis elegans1* (Cold Spring Harbor Laboratory)), pp. 1091–1105.
5. Kiontke, K., and Sudhaus, W. (2006). Ecology of *Caenorhabditis* species. WormBook. https://doi.org/10.1895/wormbook.1.37.1.
6. Hong, R.L., and Sommer, R.J. (2006). *Pristionchus pacificus*: a well-rounded nematode. BioEssays *28*, 651–659.
7. Dirksen, P., Marsh, S.A., Braker, I., Heitland, N., Wagner, S., Nakad, R., Mader, S., Petersen, C., Kowallik, V., Rosenstiel, P., et al. (2016). The native microbiome of the nematode *Caenorhabditis elegans*: gateway to a new host-microbiome model. BMC Biol. *14*, 38.
8. Samuel, B.S., Rowedder, H., Braendle, C., Félix, M.A., and Ruvkun, G. (2016). *Caenorhabditis elegans* responses to bacteria from its natural habitats. Proc. Natl. Acad. Sci. USA *113*, E3941–E3949.
9. Berg, M., Stenuit, B., Ho, J., Wang, A., Parke, C., Knight, M., Alvarez-Cohen, L., and Shapira, M. (2016). Assembly of the *Caenorhabditis elegans* gut microbiota from diverse soil microbial environments. ISME J. *10*, 1998–2009.
10. Meyer, J.M., Baskaran, P., Quast, C., Susoy, V., Rödelsperger, C., Glöckner, F.O., and Sommer, R.J. (2017). Succession and dynamics of *Pristionchus* nematodes and their microbiome during decomposition of *Oryctes borbonicus* on la Réunion Island. Environ. Microbiol. *19*, 1476–1489.
11. Renahan, T., Lo, W.-S., Werner, M.S., Rochat, J., Herrmann, M., and Sommer, R.J. (2021). Nematode biphasic "boom and bust" dynamics are dependent on host bacterial load while linking dauer and mouthform polyphenisms. Environ. Microbiol. *23*, 5102–5113.

12. MacNeil, L.T., Watson, E., Arda, H.E., Zhu, L.J., and Walhout, A.J.M. (2013). Diet-induced developmental acceleration independent of TOR and insulin in *C. elegans*. Cell *153*, 240–252.
13. Watson, E., MacNeil, L.T., Ritter, A.D., Yilmaz, L.S., Rosebrock, A.P., Caudy, A.A., and Walhout, A.J.M. (2014). Interspecies systems biology uncovers metabolites affecting *C. elegans* gene expression and life history traits. Cell *156*, 759–770.
14. Akduman, N., Lightfoot, J.W., Röseler, W., Witte, H., Lo, W.S., Rödelsperger, C., and Sommer, R.J. (2020). Bacterial vitamin B12 production enhances nematode predatory behavior. ISME J. *14*, 1494–1507.
15. O'Donnell, M.P., Fox, B.W., Chao, P.H., Schroeder, F.C., and SenGupta, P. (2020). A neurotransmitter produced by gut bacteria modulates host sensory behaviour. Nature *583*, 415–420.
16. Dieterich, C., Clifton, S.W., Schuster, L.N., Chinwalla, A., Delehaunty, K., Dinkelacker, I., Fulton, L., Fulton, R., Godfrey, J., Minx, P., et al. (2008). The *Pristionchus pacificus* genome provides a unique perspective on nematode lifestyle and parasitism. Nat. Genet. *40*, 1193–1198.
17. Herrmann, M., Mayer, W.E., and Sommer, R.J. (2006). Nematodes of the genus *Pristionchus* are closely associated with scarab beetles and the Colorado potato beetle in Western Europe. Zoology (Jena) *109*, 96–108.
18. Morgan, K., McGaughran, A., Villate, L., Herrmann, M., Witte, H., Bartelmes, G., Rochat, J., and Sommer, R.J. (2012). Multi locus analysis of *Pristionchus pacificus* on la Réunion Island reveals an evolutionary history shaped by multiple introductions, constrained dispersal events and rare out-crossing. Mol. Ecol. *21*, 250–266.
19. Riebesell, M., and Sommer, R.J. (2017). Three-dimensional reconstruction of the pharyngeal gland cells in the predatory nematode *Pristionchus pacificus*. J. Morphol. *278*, 1656–1666.
20. Bento, G., Ogawa, A., and Sommer, R.J. (2010). Co-option of the hormone-signalling module dafachronic acid–DAF-12 in nematode evolution. Nature *466*, 494–497.
21. Ragsdale, E.J., Müller, M.R., Rödelsperger, C., and Sommer, R.J. (2013). A developmental switch coupled to the evolution of plasticity acts through a sulfatase. Cell *155*, 922–933.
22. Rae, R., Riebesell, M., Dinkelacker, I., Wang, Q., Herrmann, M., Weller, A.M., Dieterich, C., and Sommer, R.J. (2008). Isolation of naturally associated bacteria of necromenic *Pristionchus* nematodes and fitness consequences. J. Exp. Biol. *211*, 1927–1936.
23. Chantanao, A., and Jensen, H.J. (1969). Saprozoic nematodes as carriers and disseminators of plant pathogenic bacteria. J. Nematol. *1*, 216–218.
24. Wei, J.Z., Hale, K., Carta, L., Platzer, E., Wong, C., Fang, S.C., and Aroian, R.V. (2003). *Bacillus thuringiensis* crystal proteins that target nematodes. Proc. Natl. Acad. Sci. USA *100*, 2760–2765.
25. Rae, R., Iatsenko, I., Witte, H., and Sommer, R.J. (2010). A subset of naturally isolated *Bacillus* strains show extreme virulence to the free-living nematodes *Caenorhabditis elegans* and *Pristionchus pacificus*. Environ. Microbiol. *12*, 3007–3021.
26. Lee, C.S., Jung, Y.T., Park, S., Oh, T.K., and Yoon, J.H. (2010). *Lysinibacillus xylanilyticus* sp. nov., a xylan-degrading bacterium isolated from forest humus. Int. J. Syst. Evol. Microbiol. *60*, 281–286.
27. Akduman, N., Rödelsperger, C., and Sommer, R.J. (2018). Culture-based analysis of Pristionchus-associated microbiota from beetles and figs for studying nematode-bacterial interactions. PLoS One *13*, e0198018.
28. Mukhopadhyay, A., and Tissenbaum, H.A. (2007). Reproduction and longevity: secrets revealed by *C. elegans*. Trends Cell Biol. *17*, 65–71.
29. Zhang, F., Berg, M., Dierking, K., Félix, M.A., Shapira, M., Samuel, B.S., and Schulenburg, H. (2017). *Caenorhabditis elegans* as a model for microbiome research. Front. Microbiol. *8*, 485.
30. Avery, L. (1993). The genetics of feeding in *Caenorhabditis elegans*. Genetics *133*, 897–917.
31. Srinivasan, V., Stedtfeld, R.D., Tourlousse, D.M., Baushke, S.W., Xin, Y., Miller, S.M., Pham, T., Rouillard, J.M., Gulari, E., Tiedje, J.M., and Hashsham, S.A. (2017). Diagnostic microarray for 14 water and foodborne pathogens using a flatbed scanner. J. Microbiol. Methods *139*, 15–21.
32. Beydoun, S., Choi, H.S., Dela-Cruz, G., Kruempel, J., Huang, S., Bazopoulou, D., Miller, H.A., Schaller, M.L., Evans, C.R., and Leiser, S.F. (2021). An alternative food source for metabolism and longevity studies in *Caenorhabditis elegans*. Commun. Biol. *4*, 258.
33. Ren, P., Lim, C.S., Johnsen, R., Albert, P.S., Pilgrim, D., and Riddle, D.L. (1996). Control of *C. elegans* larval development by neuronal expression of a TGF-beta homolog. Science *274*, 1389–1391.
34. Schackwitz, W.S., Inoue, T., and Thomas, J.H. (1996). Chemosensory neurons function in parallel to mediate a pheromone response in *C. elegans*. Neuron *17*, 719–728.
35. Savage-Dunn, C., and Padgett, R.W. (2017). The TGF-β family in *Caenorhabditis elegans*. Cold Spring Harb. Perspect. Biol. *9*, a022178.
36. Murphy, C.T., and Hu, P.J. (2013). Insulin/insulin-like growth factor signaling in *C. elegans*. Wormbook. https://doi.org/10.1895/wormbook.1.164.1.
37. Blackwell, T.K., Sewell, A.K., Wu, Z., and Han, M. (2019). TOR signaling in *Caenorhabditis elegans* development, metabolism, and aging. Genetics *213*, 329–360.
38. Meisel, J.D., Panda, O., Mahanti, P., Schroeder, F.C., and Kim, D.H. (2014). Chemosensation of bacterial secondary metabolites modulates neuroendocrine signaling and behavior of *C. elegans*. Cell *159*, 267–280.
39. Hong, R.L., Riebesell, M., Bumbarger, D.J., Cook, S.J., Carstensen, H.R., Sarpolaki, T., Cochella, L., Castrejon, J., Moreno, E., Sieriebriennikov, B., et al. (2019). Evolution of neuronal anatomy and circuitry in two highly divergent nematode species. eLife *8*, e47155.
40. Savage, C., Das, P., Finelli, A.L., Townsend, S.R., Sun, C.Y., Baird, S.E., and Padgett, R.W. (1996). Caenorhabditis elegans genes sma-2, sma-3, and sma-4 define a conserved family of transforming growth factor beta pathway components. Proc. Natl. Acad. Sci. USA *93*, 790–794.
41. Hansen, M., Flatt, T., and Aguilaniu, H. (2013). Reproduction, fat metabolism, and life span: what is the connection? Cell Metab. *17*, 10–19.
42. Riddle, D.L., Blumenthal, T., Meyer, B.J., and Priess, J.R. (1997). Life History and Evolution. In *C. elegans* II., Second Edition (Cold Spring Harbor Laboratory Press).
43. Schulenburg, H., and Félix, M.A. (2017). The natural biotic environment of *Caenorhabditis elegans*. Genetics *206*, 55–86.
44. Storelli, G., Strigini, M., Grenier, T., Bozonnet, L., Schwarzer, M., Daniel, C., Matos, R., and Leulier, F. (2018). *Drosophila* perpetuates nutritional mutualism by promoting the fitness of Its intestinal symbiont *Lactobacillus plantarum*. Cell Metab *27*, 362–377.e8.
45. Shin, S.C., Kim, S.H., You, H., Kim, B., Kim, A.C., Lee, K.A., Yoon, J.H., Ryu, J.H., and Lee, W.J. (2011). *Drosophila* microbiome modulates host developmental and metabolic homeostasis via insulin signaling. Science *334*, 670–674.
46. Consuegra, J., Grenier, T., Akherraz, H., Rahioui, I., Gervais, H., da Silva, P., and Leulier, F. (2020). Metabolic cooperation among commensal bacteria supports *Drosophila* juvenile growth under nutritional stress. iScience *23*, 101232.
47. Gilabert, A., Curran, D.M., Harvey, S.C., and Wasmuth, J.D. (2016). Expanding the view on the evolution of the nematode dauer signalling pathways: refinement through gene gain and pathway co-option. BMC Genomics *17*, 476.
48. Storelli, G., Defaye, A., Erkosar, B., Hols, P., Royet, J., and Leulier, F. (2011). *Lactobacillus plantarum* promotes *Drosophila* systemic growth by modulating hormonal signals through TOR-dependent nutrient sensing. Cell Metab. *14*, 403–414.
49. Rosshart, S.P., Vassallo, B.G., Angeletti, D., Hutchinson, D.S., Morgan, A.P., Takeda, K., Hickman, H.D., McCulloch, J.A., Badger, J.H., Ajami, N.J., et al. (2017). Wild mouse gut microbiota promotes host fitness and improves disease resistance. Cell *171*, 1015–1028.e13.
50. Rosshart, S.P., Herz, J., Vassallo, B.G., Hunter, A., Wall, M.K., Badger, J.H., McCulloch, J.A., Anastasakis, D.G., Sarshad, A.A., Leonardi, I., et al. (2019). Laboratory mice born to wild mice have natural microbiota and model human immune responses. Science *365*, eaaw4361.

51. Han, Z., Lo, W.S., Lightfoot, J.W., Witte, H., Sun, S., and Sommer, R.J. (2020). Improving transgenesis efficiency and CRISPR-associated tools through codon optimization and native intron addition in Pristionchus nematodes. Genetics *216*, 947–956.

52. Dirksen, P., Assié, A., Zimmermann, J., Zhang, F., Tietje, A.M., Marsh, S.A., Félix, M.A., Shapira, M., Kaleta, C., Schulenburg, H., et al. (2020). CeMbio – the *Caenorhabditis elegans* microbiome resource. G3 (Bethesda) *10*, 3025–3039.

53. Yarza, P., Yilmaz, P., Pruesse, E., Glöckner, F.O., Ludwig, W., Schleifer, K.H., Whitman, W.B., Euzéby, J., Amann, R., and Rosselló-Móra, R. (2014). Uniting the classification of cultured and uncultured bacteria and archaea using 16S rRNA gene sequences. Nat. Rev. Microbiol. *12*, 635–645.

54. Zerbino, D.R., and Birney, E. (2008). Velvet: algorithms for de novo short read assembly using de Bruijn graphs. Genome Res. *18*, 821–829.

55. Aziz, R.K., Bartels, D., Best, A.A., DeJongh, M., Disz, T., Edwards, R.A., Formsma, K., Gerdes, S., Glass, E.M., Kubal, M., et al. (2008). The RAST Server: rapid annotations using subsystems technology. BMC Genomics *9*, 75.

56. Emms, D.M., and Kelly, S. (2015). OrthoFinder: solving fundamental biases in whole genome comparisons dramatically improves orthogroup inference accuracy. Genome Biol. *16*, 157.

57. Kozlov, A.M., Darriba, D., Flouri, T., Morel, B., and Stamatakis, A. (2019). RAxML-NG: a fast, scalable and user-friendly tool for maximum likelihood phylogenetic inference. Bioinformatics *35*, 4453–4455.

58. Kim, D., Langmead, B., and Salzberg, S.L. (2015). HISAT: a fast spliced aligner with low memory requirements. Nat. Methods *12*, 357–360.

59. Schindelin, J., Arganda-Carreras, I., Frise, E., Kaynig, V., Longair, M., Pietzsch, T., Preibisch, S., Rueden, C., Saalfeld, S., Schmid, B., et al. (2012). Fiji: an open-source platform for biological-image analysis. Nat. Methods *9*, 676–682.

60. Rödelsperger, C., Meyer, J.M., Prabh, N., Lanz, C., Bemm, F., and Sommer, R.J. (2017). Single-molecule sequencing reveals the chromosome-scale genomic architecture of the nematode model organism *Pristionchus pacificus*. Cell Rep. *21*, 834–844.

61. Liao, Y., Smyth, G.K., and Shi, W. (2014). featureCounts: an efficient general purpose program for assigning sequence reads to genomic features. Bioinformatics *30*, 923–930.

62. Tarazona, S., Furió-Tarí, P., Turrà, D., Pietro, A.D., Nueda, M.J., Ferrer, A., and Conesa, A. (2015). Data quality aware analysis of differential expression in RNA-seq with NOISeq R/Bioc package. Nucleic Acids Res. *43*, e140.

63. Subramanian, A., Tamayo, P., Mootha, V.K., Mukherjee, S., Ebert, B.L., Gillette, M.A., Paulovich, A., Pomeroy, S.L., Golub, T.R., Lander, E.S., and Mesirov, J.P. (2005). Gene set enrichment analysis: a knowledge-based approach for interpreting genome-wide expression profiles. Proc. Natl. Acad. Sci. USA *102*, 15545–15550.

64. Schloss, P.D., Westcott, S.L., Ryabin, T., Hall, J.R., Hartmann, M., Hollister, E.B., Lesniewski, R.A., Oakley, B.B., Parks, D.H., Robinson, C.J., et al. (2009). Introducing Mothur: open-source, platform-independent, community-supported software for describing and comparing microbial communities. Appl. Environ. Microbiol. *75*, 7537–7541.

65. Brenner, S. (1974). The genetics of *Caenorhabditis elegans*. Genetics *77*, 71–94.

66. Mayer, W.E., Herrmann, M., and Sommer, R.J. (2007). Phylogeny of the nematode genus *Pristionchus* and implications for biodiversity, biogeography and the evolution of hermaphroditism. BMC Evol. Biol. *7*, 104.

67. Choi, K.H., and Schweizer, H.P. (2006). mini-Tn7 insertion in bacteria with single attTn7 sites: Example *Pseudomonas aeruginosa*. Nat. Protoc. *1*, 153–161.

68. Inoue, H., Nojima, H., and Okayama, H. (1990). High efficiency transformation of *Escherichia coli* with plasmids. Gene *96*, 23–28.

69. Kozich, J.J., Westcott, S.L., Baxter, N.T., Highlander, S.K., and Schloss, P.D. (2013). Development of a dual-index sequencing strategy and curation pipeline for analyzing amplicon sequence data on the MiSeq Illumina sequencing platform. Appl. Environ. Microbiol. *79*, 5112–5120.

70. Kuleshov, M.V., Jones, M.R., Rouillard, A.D., Fernandez, N.F., Duan, Q., Wang, Z., Koplev, S., Jenkins, S.L., Jagodnik, K.M., Lachmann, A., et al. (2016). Enrichr: a comprehensive gene set enrichment analysis web server 2016 update. Nucleic Acids Res. *44*, W90–W97.

71. Witte, H., Moreno, E., Rödelsperger, C., Kim, J., Kim, J.S., Streit, A., and Sommer, R.J. (2015). Gene inactivation using the CRISPR/Cas9 system in the nematode *Pristionchus pacificus*. Dev. Genes Evol. *225*, 55–62.

72. Stiernagle, T. (2006). Maintenance of *C. elegans*. WormBook. https://doi.org/10.1895/wormbook.1.101.1.

73. Mok, D.Z.L., Sternberg, P.W., and Inoue, T. (2015). Morphologically defined sub-stages of *C. elegans* vulval development in the fourth larval stage. BMC Dev. Biol. *15*, 26.

74. Sun, S., Rödelsperger, C., and Sommer, R.J. (2021). Single worm transcriptomics identifies a developmental core network of oscillating genes with deep conservation across nematodes. Genome Res. *31*, 1590–1601.

Please cite this article in press as: Lo et al., Synergistic interaction of gut microbiota enhances the growth of nematode through neuroendocrine signaling, Current Biology (2022), https://doi.org/10.1016/j.cub.2022.03.056

STAR★METHODS

KEY RESOURCES TABLE

REAGENT or RESOURCE	SOURCE	IDENTIFIER
Bacterial and virus strains		
Escherichia coli: OP50	Caenorhabditis Genetics Center	WBStrain00041969
Erwinia tasmaniensis NA6	Sommer Lab, Akduman et al.[27]	N/A
Erwinia toletana V100	Sommer Lab, Akduman et al.[27]	N/A
Escherichia coli: OP50-DsRed	This paper	N/A
Lysinibacillus xylanilyticus 057	This paper	N/A
Deposited data		
Pristionchus microbiome 16S rDNA sequencing	European Nucleotide Archive (ENA, https://www.ebi.ac.uk/ena), Meyer et al.[10]	PRJEB13694
The sequencing data used in this report	NCBI BioProject Database: https://www.ncbi.nlm.nih.gov/bioproject/	PRJNA752522
The sequencing data used in this report	NCBI BioProject Database: https://www.ncbi.nlm.nih.gov/bioproject/	PRJNA746221
Experimental models: Organisms/strains		
Caenorhabditis elegans: *phm-2*	*C. elegans* Genetics Center	DA597
Caenorhabditis elegans: N2: wild type	*C. elegans* Genetics Center	N/A
P. pacificus 312	Sommer Lab	N/A
P. pacificus RSB068	Sommer Lab, Morgan et al.[18]	N/A
P. pacificus RSB080	Sommer Lab, Morgan et al.[18]	N/A
Oligonucleotides		
gRNA and primers for CRISPR, see Table S2	This study	N/A
Primers for qPCR, see Table S3	This study	N/A
Recombinant DNA		
*p*UC18T-mini-Tn7T-Gm-dsRedExpress	Addgene	65032
Software and algorithms		
SILVA 16S ribosomal RNA database	Yarza et al.[53]	https://www.arb-silva.de/
Velvet	Zerbino et al.[54]	https://github.com/dzerbino/velvet
RAST Server	Aziz et al.[55]	https://rast.nmpdr.org
Orthofinder	Emms et al.[56]	https://github.com/davidemms/OrthoFinder
RAxML-NG	Kozlov et al.[57]	https://github.com/amkozlov/raxml-ng
Hisat2	Kim et al.[58]	http://daehwankimlab.github.io/hisat2/
Fiji	Schindelin et al.[59]	https://imagej.net/software/fiji/
P. pacificus reference genome	Rödelsperger et al.[60]	http://pristionchus.org
featureCounts	Liao et al.[61]	http://subread.sourceforge.net/
NOISeq	Tarazona et al.[62]	https://www.bioconductor.org/packages/release/bioc/html/NOISeq.html
Gene Set Enrichment Analysis	Subramanian et al.[63]	https://www.gsea-msigdb.org
Mothur	Schloss et al.[64]	https://mothur.org/

RESOURCE AVAILABILITY

Lead contact

Further information and requests for resources and reagents should be directed to and will be fulfilled by the lead contact Ralf J. Sommer ralf.sommer@tuebingen.mpg.de.

Please cite this article in press as: Lo et al., Synergistic interaction of gut microbiota enhances the growth of nematode through neuroendocrine signaling, Current Biology (2022), https://doi.org/10.1016/j.cub.2022.03.056

Materials availability

P. pacificus strains and bacterial isolates generated in this work are freely available through the Lead Contact.

Data and code availability

Sequencing data have been deposited at NCBI Sequence Read Archive, and accession numbers are listed in the key resources table. This paper analyzes existing, publicly available data. These accession numbers for the datasets are listed in the key resources table. This paper does not report original code. All data and codes reported in this work are freely available through the Lead Contact.

EXPERIMENTAL MODEL AND SUBJECT DETAILS

P. pacificus and *C. elegans* Strains

Nematode strains were maintained under standard laboratory conditions as described previously.[65] The *C. elegans phm-2* mutant strain was obtained from the *C. elegans* Genetics Center (CGC). The *P. pacificus* strains RSB068 and RSB080 were collected on La Réunion Island in 2011. All wild type strains were thawed from our frozen collection at the beginning of this project to avoid laboratory domestication effects.

Bacterial Culture

Bacterial liquid cultures were grown overnight in Luria-Bertani (LB) broth at 28°C and 37°C for environmental isolates and *E. coli* OP50, respectively. The environmental isolates grow faster than *E. coli* OP50 at 20°C, the temperature used to maintain nematodes. To better control the ratio and to provide a sufficient *E. coli* OP50 to support the growth of *Pristionchus*, bacterial cells from the overnight culture were pelleted by centrifuge of 2500 x g for 10 min and suspended to 0.1X of the original volume of M9 buffer. For mixed cultures, *E. coli* OP50 and the test bacterium were mixed in a ratio of 9:1. For monoxenic cultures, concentrated bacterial suspensions were directly seeded on NGM plates. Plates were incubated at room temperature for at least 24 hours before usage.

METHOD DETAILS

Bacteria Collection and Identification

Oryctes borbonicus beetles were collected from Trois Bassins on La Réunion Island in January 2018. To mimic the natural decaying process, a total of 12 beetles were sacrificed, and dissected beetles were mixed with soil, put into a mesh cage, then buried in the soil at the original collecting site at a depth of 10 cm, as described before.[10] Mesh cages were recovered after seven days and immediately brought to the laboratory. The beetle carcass and soil were transferred to 10 cm petri dishes until the emergence of nematodes. We successfully recovered *Pristionchus* populations from six samples. We collected nematodes by rinsing the carcass using M9 buffer. Subsequently, animals were washed three times to remove the bacteria attached to the surface. From each beetle carcass, at least 10 animals were pooled and grounded using TissueLyser II (Qiagen). Bacteria from the supernatant were grown on modified LB plates that contained 10% of peptone and yeast extract at 20 °C until bacterial colonies emerged. Bacterial isolates were identified by sequencing the full-length 16S rRNA gene using primers 27f (5′-AGAGTTTGATCCTGGCTCAG-3′) and 1492r (5′-GGTTACCTTGTTACGACTT-3′). *Pristionchus* species were confirmed by sequencing small subunit ribosomal RNA (SSU) gene using primer SSU18A (5′-AAAGATTAAGCCATGCATG-3′) and SSU 26R (5′-CATTCTTGGCAAATGCTTTCG-3′).[66] The plasmid pUC18T-mini-Tn7T-Gm-dsRedExpress[67] was purchased from Addgene (plasmid # 65032), and transformed into the competent cell of *E. coli* OP50 using a standard protocol.[68]

Quantification of Microbial Communities

We reanalyzed the 16S rRNA gene sequencing results from previous microbiome studies on La Réunion Island[10] to improve the taxonomic resolution. The raw reads were acquired from European Nucleotide Archive (ENA, https://www.ebi.ac.uk/ena) under the study accession PRJEB13694. Only samples whose descriptions were ‘‘Pristionchus pacificus’’, ‘‘decaying gut’’(of beetle), or ‘‘decaying soil’’ were included. We used the software Mothur[64] to cluster sequences into operational taxonomic units (OTUs) and assigned taxonomy. Raw reads were processed following the MiSeq SOP.[69] Briefly, sequences were clustered into OUTs at 97% similarity. Taxonomies were assigned using release 123 of the SILVA 16S ribosomal RNA database.[53] The taxonomies of OUTs are summarized in Data S1.

L. xylanilyticus Whole-genome Sequencing and Phylogenetic Analysis

Bacterial DNA was isolated using MasterPure Complete DNA and RNA Purification Kit (Lucigen) following the manufacturer’s instructions for DNA isolation. Illumina TruSeq Nano DNA Kit (Illumina) was used to generate the Illumina library with an average insert size of 550bps. Illumina sequencing was performed on a MiSeq that produced paired-end 2 × 300 bp reads. The genome assembly was performed using Velvet,[54] and the annotation was performed using the RAST Server.[55] To define the phylogenetic relationship, the whole genome sequences of the genus *Lysinibacillus* was downloaded from the Microbial Genomes resource of NCBI. We included genome assemblies with determined species characteristics that also had assembled genomes to scaffold level. The species tree is constructed by 106 single-copy orthogroups using software Orthofinder[56] and RAxML-NG.[57]

Paraformaldehyde Treatment of *L. xylanilyticus*

Overnight cultures of *L. xylanilyticus* were pelleted by centrifuging at 2500 × g for 10 min. Pellets were suspended using LB containing 0.5% of PFA, and the bacterial culture was shaken at 28°C for 1 hour to fix the bacterial cells. After PFA treatment, *L. xylanilyticus* was pelleted and 50mL of 1X PBS was used to wash the pellets. Washing was repeated five times, and the pellets were suspended to 0.1X of the original volume of M9 buffer. We first seeded the PFA-treated *L. xylanilyticus* on NGM plates to detect the efficiency of fixation. While PFA treatment kills the vegetative form of *L. xylanilyticus* effectively, growth of bacteria can be observed after 48 hours, which is likely resulting from the germination of spores. To minimize the effects of live cells, the PFA-treated *L. xylanilyticus* was prepared immediately before the experiments, and nematodes were cultured on PFA-treated *L. xylanilyticus* for 24 hours.

Chemotaxis Assay

Chemotaxis assays were performed as previously reported.[6] In short, to prepare test plates, we marked 10 cm NGM plates and divided them into four equal quadrants. Concentrated bacterial cultures were prepared as described above, and 20 μl of the bacterial culture for the choice assay was spotted at the opposite ends of the plate as indicated in Figure 3B. Plates were incubated at room temperature overnight before the assay. *P. pacificus* was washed three times in M9 buffer with 0.1% of Triton-X 100 and around 100 animals were placed at the opposite ends of the other quadrants (Figure 3B). For the choice between bacterial lawns, animals on each bacterial lawn were scored after 24 hours, and the animals outside the bacterial lawn were not counted. For the choice between supernatant and the cell pellets, the bacterial cells and supernatants were separated by centrifuge, and the pellet was washed three times using 1X PBS buffer. Plates were spotted immediately before the assay, and animals on each spot were scored after 4 hours.

RNA Sequencing and Data Analysis

Synchronized *P. pacificus* grown on the different bacterial cultures were washed off from NGM plates at the appropriate time points. Total RNA was extracted using Direct-Zol RNA Mini prep kit (Zymo Research) according to the manufacturer's guidelines. ~800 ng of total RNA was used as the initial input, and the mRNA was enriched using the NEBNext poly(A) mRNA Magnetic Isolation Module (NEB). The NEBNext Ultra II Directional RNA Library Prep Kit for Illumina (NEB) was used to construct the libraries. Samples were sequenced as 150 bp paired end reads on the Illumina HiSeq3000 platform (Illumina). Raw reads have been uploaded to the Sequence Read Archive (SRA) under the study accession PRJNA746221 and PRJNA752522.

We used software Hisat2 (version 2.1.0)[58] to map raw reads to the *P. pacificus* reference genome (pristionchus.org, version: El Paco[60]), featureCounts[61] to quantify transcripts base on the El Paco gene annotations V3, and NOISeq[62] to predict differentially expressed genes (DEGs) based on the non-parametric approach. We also applied Gene Set Enrichment Analysis (GSEA)[63] approach to detect the biological pathways that are differentially expressed. The collection of gene sets were obtained from WormEnrichr,[70] the genes of *P. pacificus* were assigned into corresponded categories based on their orthology with *C. elegans*, which was defined using OrthoFinder.[56] We used GSEApy (https://gseapy.readthedocs.io/en/latest/) to perform the analysis.

Generation of Transgenic Animals

A 1.5 kb region upstream region of *Ppa-daf-7.1* and *Ppa-daf-7.2* were amplified by PCR and fused with the plasmids that contained optimization of GFP (PZH008) and TurboRFP (PZH009) sequences, respectively.[51] The plasmids and PS312 genomic DNA were digested with the restriction enzyme Pst I. Subsequently, *Ppa-daf-7.1*p::GFP (10 ng/μl), *Ppa-daf-7.2*p::TurboRFP (10 ng/μl), and PS312 genomic DNA (60 ng/μl) were mixed with the undigested co-injection marker *Ppa-egl-20*p::GFP (5 ng/μl) and were injected into young adults of PS312.

Generation of P. pacificus TGF-β Pathway Mutants by CRISPR/Cas9

We generated mutant alleles using the CRISPR/Cas9 technique following the protocol described previously.[51,71] Briefly, Cas9 nuclease (0.5 μg/μl, catalog# 1081058; IDT), trans-activating CRISPR RNA (0.1 μg/μl, catalog# 1072534; IDT), guide RNA (0.056 μg/μl, CRISPR/Cas9 RNA; IDT) were mixed and injected into young hermaphrodites. Offspring harboring CRISPR-edited alleles were identified by single-worm PCR and sequenced by Sanger sequencing. The guide RNA and PCR primers used in each gene are summarized in Table S2.

qRT-PCR and qPCR

Animals and bacterial lawn preparation and RNA extraction were performed as described above. We used the iTaq Universal SYBR Green One-Step Kit (Bio-Rad Laboratories) for qRT-PCR reaction to measure gene expression in nematodes. We used *eif*-3.C and *csq*-1 genes as internal controls. For qPCR, we used iTaq Universal SYBR Green Supermix (Bio-Rad Laboratories) to quantify the ratio of bacteria. The qPCR assays were performed using LightCycler 480 Instrument II (Roche Life Science). The relative-fold changes were calculated using the $2^{-\Delta\Delta C}{}_{T}$ method. All the primers for PCR assays are listed in Table S3.

QUANTIFICATION AND STATISTICAL ANALYSIS

For the measurement of life-history traits, *P. pacificus* and *C. elegans* were grown at 20 °C. Nematodes were first synchronized by bleaching[72] and allowed to hatch in M9 buffer for 24 hours. Animals arrested at the J2 and L1 stages in *P. pacificus* and *C. elegans*, respectively. After synchronization, nematodes were transferred to NGM plates seeded with the appropriate bacterial cultures. For

body size measurement, nematodes were washed off from plates and transferred into wells of 24-well plates that containing 500 μl of M9 with 5 mM sodium azide (NaN3). Nematode images were acquired using a SteREO Discovery V12 microscope (Carl Zeiss Microscopy) with an AxioCam color camera. The sizes of nematodes were measured using the software Fiji using 'Analyze Particles' function.[59] At least 30 individuals were measured in each treatment and random sampling of 30 individuals for the following statistical analysis. For the determination of developmental growth rate, *P. pacificus* was collected and mounted on agarose pads. The age of the animal was determined based on the development of the vulva under a microscope. The development stages of *P. pacificus* resemble that of *C. elegans*. We defined the sub-stage[73,74] of L4.0 to L4.3 as early J4, L4.4 to L4.7 as middle J4, and L4.7 and L4.9 as late J4. For brood size measurement, *P. pacificus* was grown until the late J4 stage, and individual hermaphrodites were transferred to a new plate seeded with the corresponding bacterial culture. The number of offspring was counted at the juvenile stage. For longevity assays, animals were transferred using an eyelash picker every day until they stopped producing eggs, and afterwards were transfer every 5 days until the death of the animals.

For lipid staining and intensity quantification, we applied a lipid droplet staining protocol from Li and co-workers (2006) with optimization. Briefly, P. pacificus was fixed in 1% paraformaldehyde/PBS for 30 min, then immediately frozen in liquid nitrogen and thawed with running tap water. After three washing steps with 1X PBS, samples were dehydrated in 60% isopropanol for 2 min, then stained with 60% Oil-Red-O working solution for 30 min with rocking. Stained samples were washed three times with 1X PBS and mounted in 1X M9 onto agarose-padded slides for imaging. The Oil-Red-O images were acquired on a Zeiss AxioImager Z1 microscope and Axiocam 506 mono camera. The Oil Red O intensity was determined using Fiji.66 A total of 10 animals per condition were analyzed.

For all the statistics analyses, Student's t test with an adjective p value using the false discovery rate (FDR) was used to compare comparisons of the differences between the control group and experimental groups. The One-way ANOVA with Tukey HSD test is used for the compare more than three comparisons.